Journal of the Earth and Space Physics, Vol. 41, No. 4, 2016, PP. 1-12

Optical dating of Holocene lake bed sediments of the Nimbluk Plain, Khorasan, Northeast Iran: Implications for the climate change and palaeo-environment

Fattahi, M.[1*] and Walker, R.[2]

1. Associate Professor, Department of Earth Physics, Institute of Geophysics, University of Tehran, Iran
2. Department of Earth Sciences, University of Oxford, Parks Road, England

(Received: 15 Apr 2014, Accepted: 17 Feb 2015)

Abstract

We have investigated an optically stimulated luminescence (OSL) dating study in the Nimbluk lakebed in Khorasan, northeast Iran. Two samples of the lake-bed sediments from ~1 m below the land surface are successfully dated at 7.3-9.9 ka. All necessary experiments have been performed to choose the most suitable procedure for dating quartz extracts using single aliquot regeneration method (SAR). We have employed weighted histogram, unweighted histogram and central age model (CAM) for equivalent dose determination. Although, these results of the ages do not allow us to determine the timing of desiccation, the results suggest that the early part of the Holocene was much wetter than today. This provides valuable palaeo-environmental data in the region.

Keywords: Iran, Lake-bed sediments, Luminescence dating, Nimbulk Plain, OSL.

1. Introduction

Iran is a semi-arid to arid zone; 35.5% of Iran is covered by hyper-arid climate, 29.2% arid, 20.1% semi-arid, 5% Mediterranean and 10% wet. Therefore, more than 75% of the total land area of the country is dominated by an arid climate (Iran-UNFCCC, 2003; Jones et al., 2013).

Natural extreme events such as unexpected warm or cold weathers, storms, widespread dust, repeated droughts, heavy floods, and hails have occurred in Iran during the recent decade. Iran has experienced 17 major droughts during the previous 44 years. During the Past 60 years more than 6470 flood events were reported and over 42% of them occurred in the last 10 years. The areas more affected by this change are water resources, health, agriculture and environment. This requires plans to reduce the harmful effects of climate change. Increased exposure to droughts, floods and storms is already destroying development opportunities and reinforcing inequalities (Molanejad & Ranjbar, 2014). Iran national climate change office was established in January 1998 to protect the environment and to help mitigate global climate change. However, it is important to mention that climate change is not just a future scenario; but it has been a challenge for humans in this century and since ancient time. Study on the past can open the window for future. For example, looking back in time can help us better understand how droughts unfold. As instrument records exist only up to maximum 300 years, we can use paleoclimate data to supplement that instrument record. These data allow us to examine droughts that happened centuries ago. Paleoclimate records are developed from natural environmental records, such as the chemical makeup of sediments at the bottoms of the lakes. To reconstruct drought-related variables from these environmental data, we can calibrate the paleoclimate records via the instrumental records to determine how well the natural records can estimate the climate records. These can be used to define the mathematical relationship between the paleoclimate data and the climate record and use that information to produce a model. This model allows us to reconstruct climate conditions as far back as we have paleoclimate data, which can often be up to thousands of years.

The main source of extreme climate change in current century has been attributed to human being by producing unbalanced gas in the atmosphere. This has caused the green house effects. Since past, nature has

[*]Corresponding author: E-mail: mfattahi@ut.ac.ir

been responsible for climate change. The variations of the sun-earth geometry related to changes in excentricity, (100 ka), obliquity (40 ka) and precession of the earth's orbit (23 ka) during the Milankovitch chron (Fig. 1), has correlated with the timing of climate change (Berger, 1994). The so-called Dansgaard-Oeschger events (Dansgaard et al., 1993; Johnsen et al., 1992), the Heinrich events or the 8.2 ka event (Rohling and Pälike, 2005) are some other natural effects. While global event during quaternary have been identified mainly using Oxygen isotope values ($\delta^{18}O$) of deep sea sediments and ice cores, evidence of Pleistocene and Holocene climate fluctuations in Iran has been documented in different geomorphic systems. Erosion physical features such as dry riverbeds, alluvial fans, sand dunes, and aeolian deposits all give clues to environmental changes. The extent and level of lakes (e.g., Van Zeist and Wright, 1963; Kelts and Shahrabi, 1986; Djamali et al., 2008; Ramezani et al., 2008), and playas or kavirs (Krinsley, 1970) have also been widely studied as indicators of climatic fluctuations. Pollen and other organisms associated with lake sediments can be used to trace changing conditions to analyze historical records. There have been some studies on past climates in some parts of Iran, attempting to link climate with past environmental conditions in the Late Pleistocene-Holocene. Although, few palaeoclimate proxy data exist for the Holocene in Iran and mainly from palynological analysis of sediment cores from Lakes (Kehl, 2009), the most complete records of climate change in Iran come from lake cores from the north-west Zagros (Jones et al., 2013), i.e. lakes Zeribar, Mirabad (e.g. vanZeist and Botema, 1977; Griffiths et al., 2001; Stevens et al., 2001, 2006), and Urmia (e.g. Bottema, 1986).

Dry lake basins are a prominent feature on the geography of the desert interior of Iran. They have the potential to contain information on the past changes in the environment of this presently extremely arid region. The timing of lake formation and desiccation in eastern Iran are, however, not well constrained at present.

Walker and Fattahi (2011) built a scenario of evolution of the landscape of eastern Iran through the Holocene using the information of published papers. Due to the importance of lakebed deposition in Nimbulk Plain, they referred to an abstract presented in a meeting in Oxford and reported the brief information of one OSL sample taken from that region. We collected another sample from the same region in a different place. The focus of our study is the Nimbluk valley, which is one of several enclosed basins within Khorasan province in northeast Iran. We provide the results of these two OSL samples. However, given the overall scarcity of palaeo-environmental studies in the interior of Iran, these ages constraint provide useful insight into the environmental changes shaped the landscape.

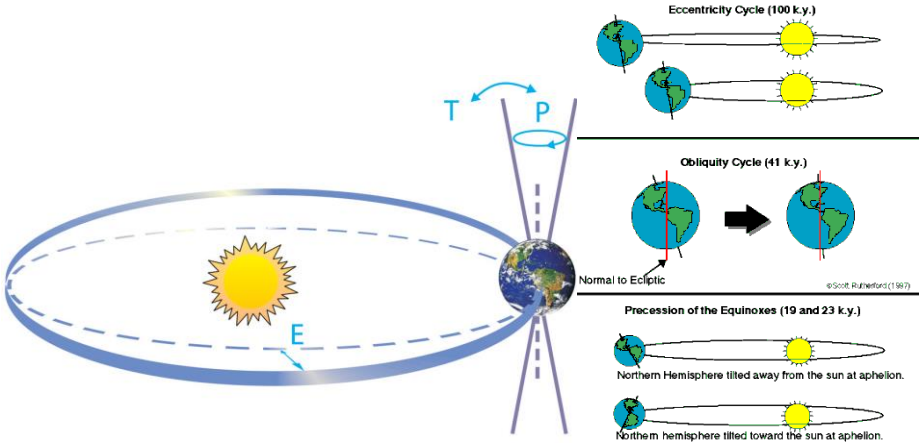

Fig. 1. Schematics of Milankovitch cycles. Milankovitch cycles describe the changes in the way the earth orbits the sun. These changes define the sequence of ice ages and warm periods. 'E' denotes eccentricity (The earth's orbit changes from being nearly circular to slightly elliptical). This cycle is affected by other planets in the solar system and has a period of around 100,000 years. 'T' denotes obliquity (The angle of tilt of the earth's axis changes from 22.1° to 24.5°). This cycle has a period of 41,000 years. 'P' denotes precession (changes in the direction of the axis tilt at a given point of the orbit). Source: Rahmstorf and Schellnhuber (2006).

Eastern Iran is a land of high mountains surrounded by inhospitable desert depressions. The extremely arid environment across much of the country forces most of the population to inhabit relatively in the narrow fringes of land flanked by high mountains on the one side and by barren desert on the other. Even at the desert margins, the rivers are dry except during rare floods, and agriculture has relied on the Qanat, tapping and distribution of scarce groundwater supplies.

The morphology of eastern Iran was resulted from active faulting and mountain building associated with the Arabia-Eurasia continental collision. Central Iran is moving northwards relative to western Afghanistan at a rate of 16 ± 2 mm/yr (Vernant et al., 2004). This has produced north-south, right-lateral shear in south part of latitude 34°N that surround Dasht-e-Lut (e.g., Walker and Jackson, 2004; Walker et al., 2004; Meyer and Le Dortz, 2007) and east-west, left-lateral, faults that are thought to rotate clockwise around a vertical axis (Jackson and McKenzie, 1984) in north latitude 34°N. The most prominent features of the left-lateral faults are the Doruneh and Dasht-e-Bayaz. The Nimbluk basin has been formed as a consequence of thrust faulting and mountain-building around the Dasht-e-Bayaz fault– the main strand of which cuts through the northern part of the basin (Fig. 2).

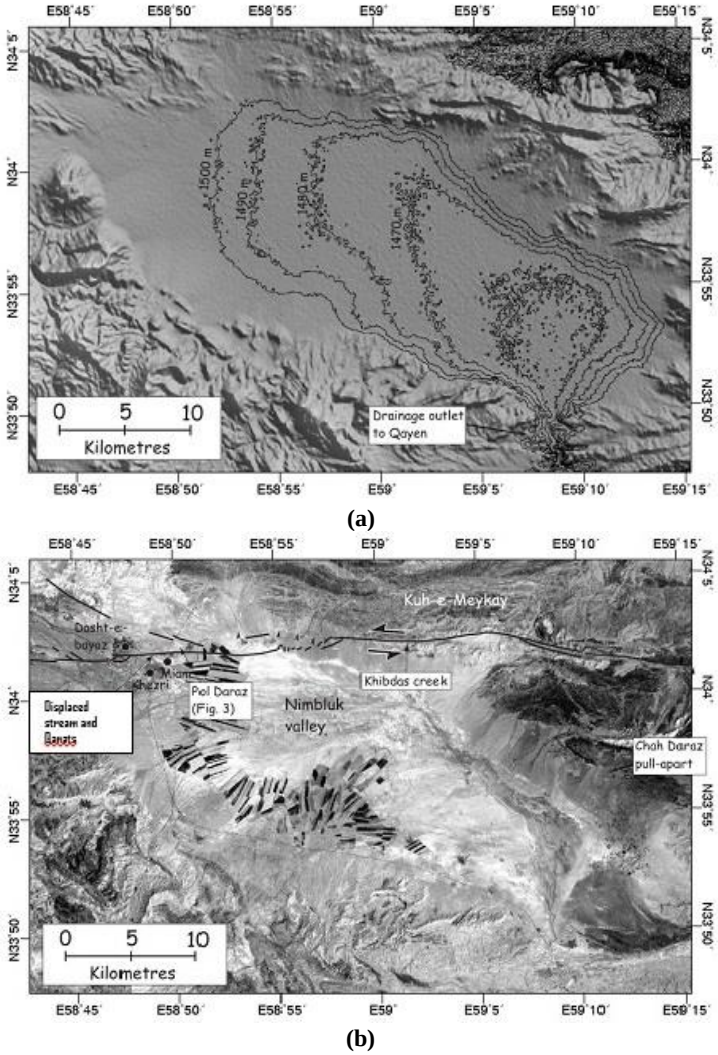

Fig. 2. (a) Shaded-relief SRTM digital topography of the Nimbluk valley. Contours at 10 m intervals are shown for elevations of 1500 m and less. Drainage within the Nimbluk valley flows southwards to Qayen through a narrow canyon. (b) LANDSAT satellite image (band 5) of the same area as in Fig. 2a is shown with ruptures of the Dasht-e-Bayaz earthquake in 1968 (Ambraseys and Tchalenko, 1969; Tchalenko and Ambraseys, 1970; Tchalenko and Berberian, 1975; Berberian, 1976). Light-coloured regions in the valley are outcrops of lakebed sediments. The lakebeds are rimmed by agricultural regions in the area east and southeast Khezri. The margins of the valley are composed of alluvial fans originating from the surrounding mountains. The locations of the Pol Daraz sampling sites are labeled (Fig. 3).

2. Landscape development in the Nimbluk valley

Digital topography and LANDSAT satellite imagery of the Nimbluk valley and its surroundings are shown in Figure 2. The low-relief base of the valley is ~30 km wide in a WNW-ESE direction and 15 km wide in a NNE-SSW direction. The base of the valley is not completely flat and there is ~40 m of relief from the lowest elevation point to the margin of lakebed exposure (Fig. 2a). Alluvial fan deposits cover the margins of the valley. Central parts of the valley are covered by light-coloured lakebed marls (visible as light colours in the LANDSAT image; Fig. 2b). A narrow band of agriculture runs along the transition between alluvium and lakebed sediments. Although lakebed deposits outcrop across the major part of the valley, the basin is not closed at the present-day; with drainage instead flowing southwards through a narrow canyon towards the town of Qayen (Fig. 2a). We suspect, therefore, that the Nimbluk basin was once closed, allowing the formation of a lake, which at some point spilled southwards to re-establish an outlet for the drainage.

3. Optically-stimulated luminescence (OSL) dating of the Nimbluk lake-bed sediments

In the north part of the village of Khezri, immediately to the east part of the main Qayen to Gonabad road, sediments of the Nimbluk palaeo-lake are exposed at Pol Daraz (Fig. 3a). Pol Daraz is a low table land, ~8 m higher than the rest of the Nimbluk valley, where it has been uplifted by a small component of vertical slip on the Dasht-e-Bayaz fault.

We collected two samples for OSL dating. A sample of lake-bed sediments (Fig. 3b) was extracted as a single large block with dimensions of ~30 cm on each side from a vertical exposure of fine-grained and homogeneous lake-bed sediments (the location of this sample, DB1, is 34:02:02.4 N; 58:49:56.6 E; Altitude 1540 m, see Fig. 3b). Another sample was collected by driving 50-mm-diameter opaque satinless steel tube into cleaned lake deposit (the location of this sample, DB2, is 34:02:04.0N; 58:49:51.2E; 1554 m; Fig. 3c). Both samples were covered by black plastics and transferred to the dark room in the Institute of Geophysics.

Under subdued red light in the laboratory, the outside, with light exposed, some parts of the block sample, DB1, were trimmed and removed. Two centimetres from both sides of tube sample, DB2, which could be exposed to light was separated and used for moisture measurement. The rest was used for equivalent dose determination. A portion of both samples were wet-sieved to separate the 90-150 μm grains and immersed for two days in 1 N HCl to remove carbonate, followed by one day immersion in H_2O_2 to remove organic material. The procedure was followed by heavy liquid separation. The grains were then treated with 48% Fluorosilicic acid for 45 min in order to remove feldspar. The quartz separates were mounted as a monolayer (approximately 5 mg/disc) on 10 mm diameter aluminium discs (aliquot) using a silicon spray as adhesive.

All the experiments reported here were carried out in Oxford University luminescence lab using a Risø (Model TL/OSL-DA-15) automated TL/OSL system (fitted with a90Sr/90Y beta source delivering ~5 Gyr min^{-1}) equipped with a blue (= 470 nm) diode array(p = 24 mW cm^{-2}) as stimulation sources. The intensity of light incident on the sample was about 400mWcm^{-2}. OSL was detected using an Electron Tubes bi-alkaline PMT. Luminescence was measured through 7 mm Hoya U-340 filters.

Quartz grains were dated with OSL using the single aliquot regenerative-dose (SAR) protocol (Table 1). SAR (Murray and Wintle, 2000) uses the luminescence signal from a test dose administrated after the regeneration dose luminescence measurement to monitor, and then correct for, any sample sensitivity changes during the measurement process. The fundamental assumption in SAR protocol is that if a plot of regeneration dose OSL (Lx) vs. test dose OSL (Tx) shows a straight line that passes through the origin, the sensitivity-correction procedure will work properly. We checked sensitivity changes of the quartz extraction of the sample, DB1, by repeated (8 times) cycles in SAR procedure with a repeated fixed regeneration and test dose. It showed a linear relationship which passed through the origin.

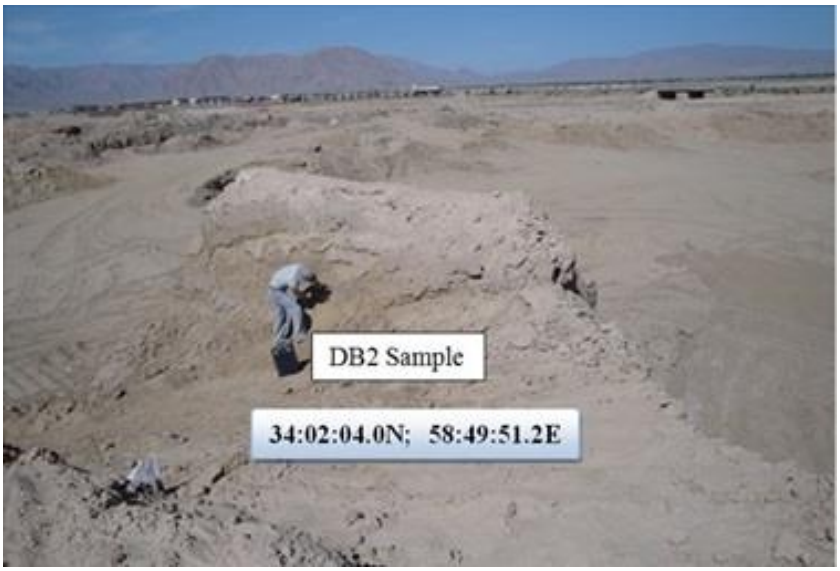

(a)

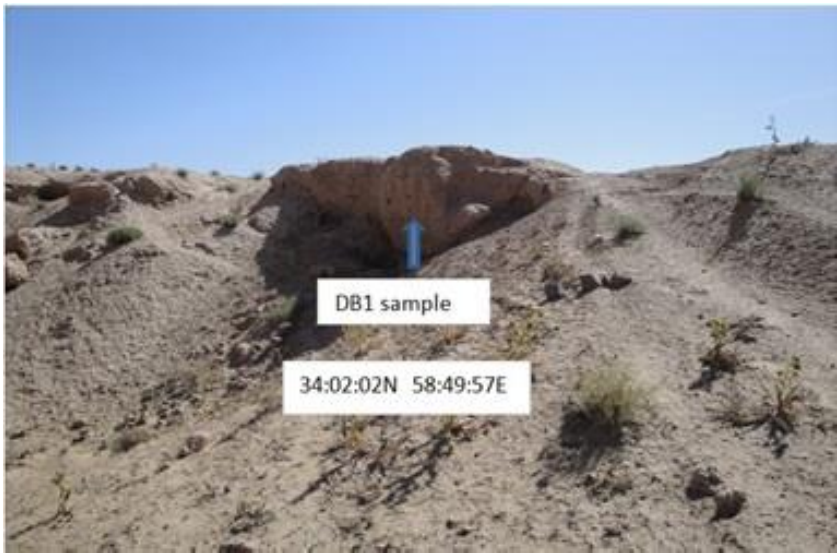

(b)

Fig. 3. (a) Field Photograph shows lake-bed sediments of the Nimbluk basin at Pol Daraz and the mountain in the distance as scale. It also shows the DE2 OSL sample location (b) Field photograph shows an exposure of fine-grained fluvial deposits at the DE1 OSL sampling location. The height of the fault scarp is ~8 m (see figures in the distance for scale). The DE1 was taken from the wall of a small excavation into the scarp.

Table 1. Generalized single aliquot regenerated sequence and outline of the steps involved in the SAR method. *Observed Lx and T_x are derived from the initial IRSL signal (2 s) minus a background estimated from the last part of the stimulation curve. In corrected natural signal $N= L_0/T_0$; in corrected regenerated signal $R_x=L_x/T_x$ (x=1-5). Note that in step 2, the sample has been heated to the pre-heat temperature using TL and held at that temperature for 10 s.

Step	Treatment 1	*Ob
1	Give dose	_
2	Pre-heat (TL 200-300ºC)	_
3	Stimulation (at 120ºC)	L_x
4	Give test dose	_
5	Cut-heat (TL 120-260ºC)	_
6	Stimulation (at 125ºC)	T_x
7	Return to 1	_

To investigate the saturation of luminescence signal of sample, DB1, the SAR protocol using 9 different regenerative doses were performed. It is clear from Figure 4 that a natural dose of >100 Gray (Gy) could be accurately measured before saturation. To test thermal transfer of charge into the OSL traps as a result of preheating (e.g., Rhodes, 2000), the natural aliquots were stimulated at room temperature and OSL was measured for 100 sec, with more than 4 hours delay between stimulations (to empty the rapidly bleaching test). Very low OSL signal (2% of the natural) was observed for the second measurement. This suggests that thermal transfer is not an effective source of uncertainty in these aliquots.

Dose recovery tests were carried out to provide a method to determine whether the overall effects of sensitivity changes had been properly corrected for. Three aliquots of sample, DB1, were used for each preheat or cut heat temperature. After depleting the natural signal, each aliquot was given ~24.66 Gy of beta dose and this dose was measured using the SAR procedures. Cut heat was initially fixed at 220ºC for 10 s and pre-heat had changes between 200 to 300ºC. Then, the pre-heat was fixed at 260ºC and the cut heat varied between 120-260ºC. The SAR procedure successfully recovered the lab dose at different temperatures (Fig. 5).

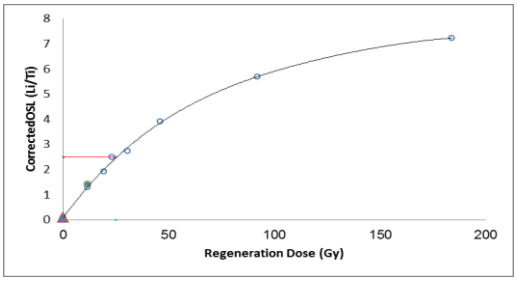

Fig. 4. Growth curve with Natural OSL decay curve. The first regenerative dose was repeated in the end of measurement (filled circle). Recuperation is close to zero and is shown as filled triangle. The test dose was 7 Gy. The natural OSL decay curve is shown inset. Error bars are too small to show.

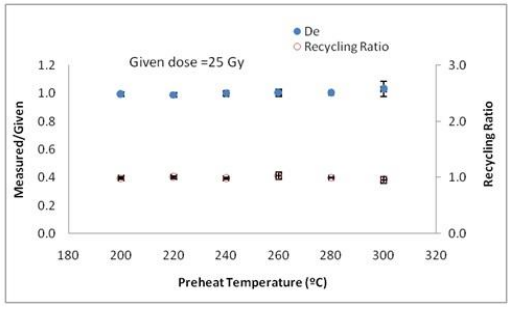

(a)

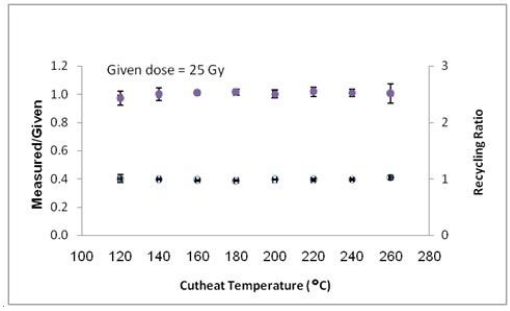

(b)

Fig. 5. Dose recovery test. (a) The cut heat was fixed at 220ºC and sample temperature was 125ºC. (b) The pre heat was fixed at 260ºC and sample temperature was 125ºC. The ratio of measured to given dose is shown as filled circles and the recycling ratios (R5/R1) of each temperature as open circles. Error bars are too small to show.

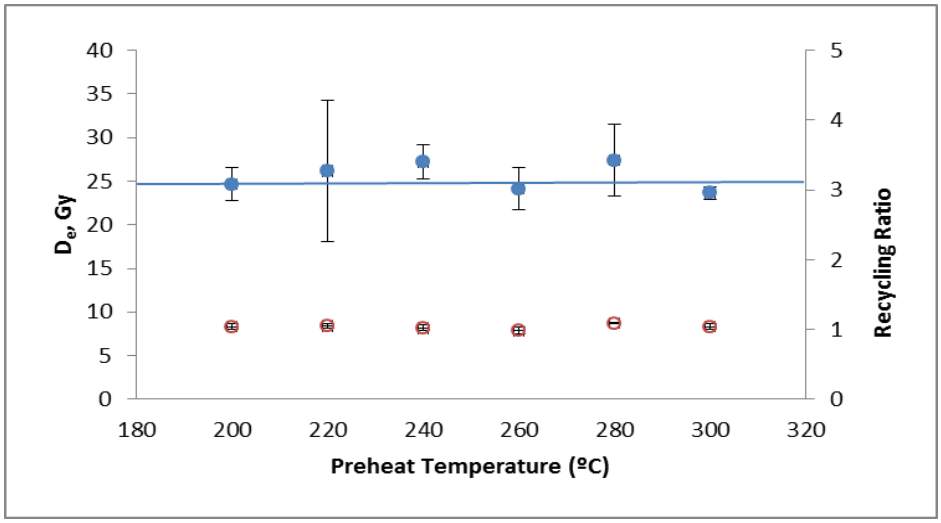

Fig. 6. Plot of equivalent dose as a function of pre-heat temperature. (a) The cut heat was fixed at 220ºC and sample temperature was 125ºC. The line is presented to show the accepted value of D_e (24.7 ± 2.7 Gy) for age determination. The scattering of De measured for each pre-heat temperature is shown by large variability in the error bars. The Equivalent doses are shown as filled circles and the recycling ratios (R5/R1) of each temperature as open circles.

The average ratios of observed to given dose for preheat platue and cut heat platue were 1.002±0.020 and 1.003±.036, respectively. These results showed that the overall effects of sensitivity changes (arising from possible changes in both electron trapping and luminescence recombination probabilities) are corrected. To determine the appropriate thermal pre-treatments in the SAR (Table 1), pre-heat platue was carried out. Figure 6 shows an apparently constant De in the temperature range 200-300ºC with the relevant recycling ratios (R5/R1) close to unity (Average 1.036 ± 0.036) for sample, DB1. Based on the above experiments, a pre-heat temperature of 260ºC (Step 2 in Table 1) and a cut heat of 220° (Step 5 in Table 1) were selected for De determination.

Twenty two and Twenty six medium size aliquots of samples, DB1 and DB2, respectively, were prepared and measured using the optimised SAR protocol. Following the measurement of the naturally acquired dose, a dose-response curve was constructed from five dose points including three regenerative doses (8, 16 and 26 Gy), and a zero dose. A replicate measurement of the lowest regenerative dose was carried out at the end of each SAR cycle. The first 2 seconds of the OSL decay curve was used for the signal, and the final 15 s of the OSL decay curve was used as a background for all measurements. The D_e was determined by interpolation and the sensitivity was corrected by dividing L_x by T_x.

No aliquot produced significant recuperation signals and all produced recycling ratios between 0.90 and 1.10. Figure 7 shows the equivalent dose measurement of sample, DB1, as the total radiation dose required to replicate the natural OSL signal. This is calculated by three statistical methods using Analyst for each of the aliquots. The results using the histogram, weighted histogram, and radial plot are similar but not identical (294.5 ± 36.77 s, 301.7 ± 38.79 s, and 299.39 ± 7.76 s). The tight clustering of equivalent dose measurements suggests that the assumption of complete solar resetting on deposition is valid in this case.

The dose rate was calculated from ICP mass spectrometer measurements of U, Th and ^{40}K for the sample DB1. The dose rate for the sample DB2 was calculated from the data acquired by field gamma spectroscopy. Full preparatory and analytical procedures are described in Fattahi et al. (2006). The total dose rate (from U, Th and ^{40}K content and corrections for cosmic ray and moisture contents) was calculated and presented in Table 2.

The calculated mean OSL age for the lake-bed samples using the equivalent doses provided by different statistical methods is presented in Table 3. The minimum and maximum ages provided by all methods are 7.3 and 9.9 ka, respectively.

Table 2. The values used to calculate annual dose rate from Dasht-e-Bayaz, northeast Iran. Uncertainties are based on the propagation, in quadrature, of errors associated with individual errors for all measured quantities.

Sample	*Grain (μm)*	*Water (%)*	*Depth (m)*	*K (%)*	*U (ppm)*	*Th (ppm)*	*Cosmic (Gy/ka)*	*Dose rate (mGy/yr)*
DB1	***90-150***	***5***	***1.25***	***1.42 ± 0.01***	***3.2 ± 0.01***	***7.20 ± 0.01***	***0.21 ± 0.13***	***2.82 ± 0.16***
DB2	***90-150***	***5***	***1.5***	***1.27 ± 0.01***	***2.03 ± 0.1***	***6.88 ± 0.1***	***0.22 ± 0.13***	***2.38 ± 0.15***

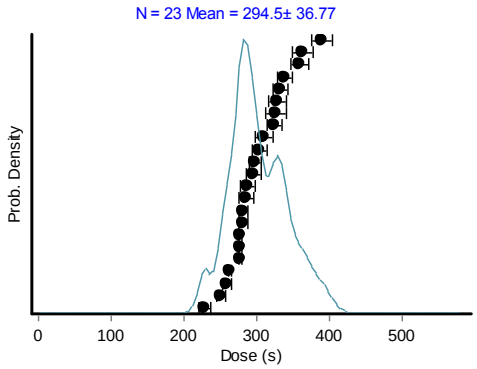

(a)

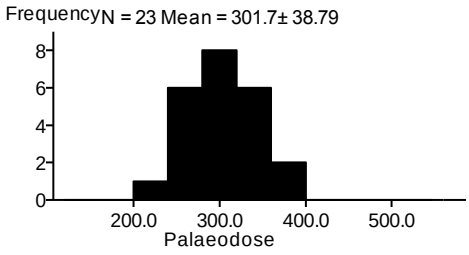

(b)

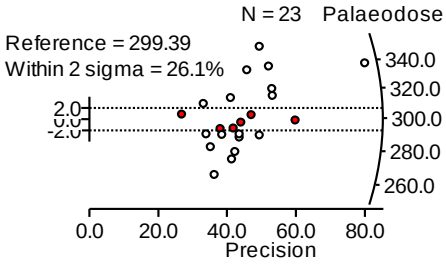

(c)

Fig. 7. Dose distribution diagrams for 23 aliquots of quartz grains from the Pol Daraz sample presented in (a) (as a weighted histogram), (b) (as a Histogram) and (c) (as radio plot) figures. The x-axis for above and middle figures is in seconds of exposure to a beta source delivering a dose of ~5 Gy per minute (see Fattahi et al., (2006) for further details).

Table 3. The values used to calculate luminescence ages employed three different statistical methods, weighted mean, Unweighted mean, and Central age model.

	De (Gy)	±	*Total (Gy/ka)*	±	*Age (ka)*	±
Weighted DB1	23.9	3.1	2.8	0.2	8.5	1.2
Unweighted DB1	24.5	3.2	2.8	0.2	8.7	1.2
CAM DB1	24.3	1.0	2.8	0.2	8.6	0.6
Unweighted DB2	21.4	1.7	2.4	0.2	9.0	0.9

4. Implications for the palaeoenvironment of NE Iran

Although being one of the hottest and most arid regions on the Earth at present, the landscape of eastern Iran retains evidence that a much milder and wetter environment existed at times in the geologically recent past.

Last glacial maximum (LGM) was windy and arid in Northeast Iran. This is evident by 12 m loess deposition at Kalate Naderi between ~26-14 ka BP (Karimi et al., 2011); and cold and dry in Ardakan, central Iran, based on the accumulation of 25 m aeolian sand-ramp during ~28.0-18.8 ka BP (Thomas et al., 1997). The final loess deposition lasted until the Early Holocene. This is based on youngest OSL ages around 10 ka in north Iran (Frechen et al., 2009) and around 12 ka in northeast Iran (Karimi et al., 2011). As there is a common acceptance of the close relationship between loess accumulations with dry-cold period, these suggest that the dry period is possibly ended around 10 ka BP in north-northeast Iran.

Therefore, the results of this research have implications for the environmental conditions in eastern Iran in the early Holocene: a region that has very little palaeoclimatic information. The OSL age of 7.3-9.9 ka for lake-bed deposits in the Nimbluk valley show that there was a substantial amount of water in a region that is now arid. We do not have a constraint on the age of the uppermost lake-beds and so do not know the exact age at which the lake desiccation occurred. In addition, we suspect from the morphology of the Nimbluk basin that the desiccation occurred at a time of elevated lake-level, when the waters were able to spill over the enclosing mountains and establish an outlet towards the south. Thus, even if we were able to constrain the age of desiccation we would not be able to constrain the timing of aridification.

However, despite the limitations described above, our data do appear to show that this part of Iran was much wetter in the early part of the Holocene than it is at present. This is also supported by the findings of Walker et al. (2010) and Fattahi et al. (2014). They also suggested that the dry lake bed in south Golbaft, central east Iran was possibly wetter than today in early to mid-Holocene.

Given the considerable apparent changes in landscape over the last 10 ka, it is possible that important developments in human society within eastern Iran occurred under climatic and environmental conditions that were very different from those seen at the present (Fouache et al., 2008; Schmidt et al., 2011). Climatic records (obtained from cave carbonates- collectively termed speleothems) in the eastern Mediterranean and Arabian regions, despite occurring under very difficult climatic regimes, show similar trends towards arid conditions from a peak in rainfall at 7-8 ka (Bar-Matthews et al., 1997; Fleitmann et al., 2007).

It is worthwhile considering how changes in the Holocene environment might affect the landscape of eastern Iran. There are few quantitative age data on Holocene landscape features from NE Iran. Fattahi et al. (2006) date the abandonment of alluvial fans at Sabzevar (~36°15'N) to ~9-13 ka. Fattahi et al. (2007) date an entrenched fan and two incised terraces of the Shesh Taraz river on the Doruneh fault (~35°15'N) to 10.6 ± 1.3 ka, 8.2 ± 2.8 ka, and 7.9 ± 3.1 ka. Both of these studies suggest changes in river hydrology and incision in the early Holocene. A separate study from Minab and Jiroft in southern Iran (~27-28°N; Regard et al., 2006) also finds periods of terrace development and fluvial incision in the early Holocene (12.8 ± 1.0 ka, 8.4 ± 1.0 ka, and 5.6 ± 0.6 ka). More recently the abandonment of an alluvial fan near Anar in central Iran to a maximum of 9.4 ka was constrained. The apparent correlation between the periods of abandonment of alluvial fans and river terraces, and the deposition of lakebed sediments, in presently dry regions, may indicate that the periods of alluvial fan abandonment and river terrace development are a response to variations in aridity. Further dating studies in Iran are required to clarify whether this correlation is real. The sedimentary records of lakes and playas in western and eastern Iran and loess-soil sequences in north and central Iran have also shown a strong potential to identify climate signals. However, more studies including high-resolution sampling and dating of these records can provide more detailed information of past climates in Iran.

Acknowledgements

We would like to thank Mohammad Madhi Khatib, Mohammad Zarrinkoub and the University of Tehran, the University of Birjand, and the Geological Survey of Iran for their support of our work. We also thank the Leverhulme Trust for funding the project. The first author thanks the flight expenses support of University of Tehran under grant number 6201002/1/10.

References

Ambraseys, N. N. and Tchalenko, J. S., 1969, The Dasht-e-Bayaz (Iran) earthquake of August 31, 1968, A field report, Bulletin of the Seismological Society of America, 59, 1751-1792.

Bar-Matthews, M., Ayalon, A. and Kaufman, A., 1997, Late quaternary paleoclimate in the Eastern Mediterranean region from stable isotope analysis of speleothems at Soreq cave, Israel. Quat. Res., 47, 155-168

Berberian, M., 1976, Contribution to the seismotectonics of Iran (Part II), Report No. 39, Geological Survey of Iran.

Berger, W. H., 1994, Quaternary fourier stratigraphy: orbital templates and Milankovitch anomalies, In: Math, Geol. 26, 769-781. Doi: 10.1007/BF02083116

Botema, S., 1986, A late quaternary pollen diagram from Lake Urmia (north western Iran), Review of Palaeobotany and Palynology, 47, 241-61.

Dansgaard, W., Johnsen, S. J., Clausen, H. B., Dahl-Jensen, D., Gundestrup, N. S., Hammer, C. U., Hvidberg, C. S., Steffensen, J. P., Sveinbjörnsdottir, A. E., Jouzel, J. and Bond, G., 1993, Evidence for general instability of past climate from a 250-kyr ice-core record, In: Nature 364, 218-220, Doi:10.1038/364218a0

Djamali, M., de Beaulieu, J.-L., Shah-hosseini, M., Andrieu-Ponel, V., Ponel, P., Amini, A., Akhani, H., Leroy, S. A. G., Stevens, L., Lahijani, H. and Brewer, S., 2008, A late pleistocene long pollen record from Lake Urmia, Iran, In: Quat. Res., 69, 413-420, Doi:10.1016/j.yqres.

Fattahi, M., Walker, R., Hollingsworth, J., Bahroudi, A., Nazari, H., Talebian, M., Armitage, S. and Stokes, S., 2006, Holocene slip-rate on the Sabzevar thrust fault, NE Iran, determined using optically stimulated luminescence (OSL), Earth and Planetary Science Letters, 245, 673-684.

Fattahi, M., Walker, R. T., Khatib, M. M., Dolati, A. and Bahroudi, A., 2007, Slip-rate estimate and past earthquakes on the Doruneh fault, eastern Iran, Geophysical Journal International, 168, 691-709

Fattahi, M., Walker, R. T., Talebian, M., Sloan, R. A. and Rasheedi, A., 2014, Late quaternary active faulting and landscape evolution in relation to the Gowk Fault in the south Golbaf Basin, S.E. Iran, Geomorphology, 204, 334-343.

Fleitmann, D., Stephen, J., Burnsb, A. M., Mudelseed, M., Kramersa, J., Villaa, I., Neffc, U., Al-Subbarye, A. A., Buettnera, A., Hipplera, D. and Matter, A., 2007, Holocene ITCZ and Indian monsoon dynamics recorded in stalagmites from Oman and Yemen (Socotra), Quat. Sci. Revs., 26, 170-188

Frechen, M., Kehl, M., Rolf, C., Sarvati, R. and Skowronek, A., 2009, Loess chronology of the Caspian Lowland in Northern Iran, Quaternary International, 198, 220-233.

Fouache, E., Cosandey, C., Adle, C., Casanova, M., Francfort, H. P., Madjidzadeh, Y., Tengberg, M., Sajadi, M., Shirazi, Z. and Vahdati, A., 2008, A study of the climatic crisis of the end of the third Millenium BC in southeastern Iran through the lens of geomorphology and archaeology, Proceedings of the 10thAnnual Symposium on Iranian Archaeology, Bandar Abbas, Iran.

Griffiths, H. E.; Schwalb, A. and Stevens, L., 2001, Environmental change in southwestern Iran: the Holocene ostracod fauna of Lake Mirabad, In: The Holocene, 11, 747-764. Doi: 10.1191/09596830195771

Iran-UNFCCC, 2003, Initial national communication report of Iran to UNFCCC (United nation framework convention on climate change) in 2003.

Jackson, J. and McKenzie, D., 1984, Active tectonics of the Alpine-Himalayan belt between Turkey and Pakistan, Geophysical Journal of the Royal Astronomical Society, 77, 185-264.

Johnsen, S. J., Clausen, H. B., Dansgaard, W., Fuhrer, K., Gundestrup, N., Hammer, C. U., Iversen, P., Jouzel, J.,

Stauffer, B. and Steffensen, J. P., 1992, Irregular glacial interstadials recorded in a new Greenland ice core, Nature, 359, 311-313, Doi:10.1038/359311a0.

Jones, M., Djamali, M., Stevens, L., Heyvaert, V., Askari, H., Noorollahi. D. and Weeks, L., 2013, Mid-Holocene environmental and climatic change in iran, Environment, ecology, landscape and subsistence ancient Iran and its neighbours, Local Developments and Long-range interactions in the 4th Millennium BC ISBN: 9781782972273 Oxbow Books Series, The British Institute of Persian Studies Archaeological Monographs Series III.

Karimi, A., Frechen, M., Khademi, H., Kehl, M. and Jalalian, A., 2011, Hronostratigraphy of loess deposits in northeast Iran, Quaternary International, 234, 124-132.

Kehl, M., 2009, Quaternary climate change in Iran, Erdkunde, 63(1), 1-17.

Kelts, K. and Shahrabi, M., 1986, Holocene sedimentology of hypersaline Lake Urmia, northwestern Iran, In: Palaeogeogr, Palaeoclimat, Palaeoecol, 54, 105-130.

Krinsley, D. B., 1970, A geomorphological and paleoclimatological study of the playas of Iran, US Geol. Surv., Contr. No. PRO CP 70-800. Washington, D.C.

Molanejad, M. and Ranjbar, A., 2014, Climatic extreme events over Iran, Observation and future projection, 3rd Meeting of COMSATS' International Thematic Research Group on 'Climate Change and Environmental Protection' (Islamabad, Pakistan).

Meyer, B. and Le Dortz, K., 2007, Strike-slip kinematics in Central and Eastern Iran, estimating fault slip-rates averaged over the Holocene, Tectonics, 26, TC5009, doi: 10.1029/2006TC002073.

Murray, A. S. and Wintle, A. G., 2000, Luminescence dating of quartz using an improved single-aliquot regenerative-dose protocol, Radiat. Meas, 32, 57-73.

Rahmstorf, S. and Schellnhuber, H. J., 2006, Der Klimawandel, Beck Verlag, Munich, 144 pp.

Ramezani, E., Marvie Mohadjer, R. M., Knapp, H.-D., Ahmadi, H. and Joosten, H., 2008, The late-Holocene vegetation history of the Central Caspian (Hyrcanian) forests of northern Iran, in: The Holocene, 18, 307-321, Doi: 10.1177/0959683607086768.

Rohling, E. J. and Pälike, H., 2005, Centennial-scale climate cooling with a sudden cold event around 8,200 years ago, in: Nature, 434, 975-979, Doi: 10.1038/nature03421

Regard, V., Bellier, O., Braucher, R., Gasse, F., Bourles, D., Mercier, J, Thomas, J-C., Abbassi, M. R., Shabanian, E. and Soleymani, Sh., 2006, 10Be dating of alluvial deposits from Southeastern Iran (the Hormoz Strait area), Palaeogeography, Plaeoclimatology, Palaeoecology, 242, 36-53.

Rhodes, E. J., 2000, Observations of thermal transfer OSL signals in glacigenic quartz, Radiation Measurements, 32, 595-602.

Schmidt, A., Quigley, M., Fattahi, M., Azizi, G., Maghsoudi, M. and Fazeli, H., 2011, Holocene settlement shifts and palaeoenvironments on the Central Iranian plateau, disentangling linked systems, The Holocene, 21(4), 583-595.

Stevens, L.; Wright, H. E. and Ito, E., 2001, Proposed changes in seasonality of climate during the Late glacial and Holocene at Lake Zeribar, Iran, in: The Holocene 11, 745-755, Doi: 10.1191/09596830195762

Stevens, L. R., Ito, E., Schwalb, A. and Wright, H. E. Jr., 2006, Timing of atmospheric precipitation in the Zagros Mountains inferred from a multi-proxy record from Lake Mirabad, Iran, in: Quat. Res., 66, 494-500, Doi:10.1016/j.yqres.2006.06.008.

Tchalenko, J. S. and Ambraseys, N. N., 1970, Structural analysis of the Dasht-e-Bayaz (Iran) earthquake fractures, Geological Society of America Bulletin, 81, 41-60.

Tchalenko, J. S. and Berberian, M., 1975, Dasht-e-Bayaz fault, Iran, earthquake and earlier related structures in bed-rock, Geological Society of America Bulletin, 86, 703-709.

Thomas, D. S. G., Bateman, M. D., Mehrshahi, D. and O'Hara, S. L., 1997, Development and environmental significance of an eolian sand ramp of last-glacial age, Central Iran, Quaternary Research, 48, 155-161.

Van Zeist, W. and Bottema, S., 1977,

Palynological investigations in Western Iran, in: Palaeohistoria, 19, 19-86, Doi: 10.1126/science.140.3562.65.

Van Zeist, W. and Wright, H. E., 1963, Preliminary pollen studies at Lake Zeribar, Zagros Mountains, south-western Iran, Science, 140, 65-67.

Vernant, P., Nilforoushan, F., Hatzfeld, D., Abassi, M. R., Vigny, C., Masson, F., Nankali, H., Martinod, J., Ashtiani, A., Bayer, R., Tavakoli, F. and Chery, J., 2004, Present-day crustal deformation and plate kinematics in the Middle East constrained by GPS measurements in Iran and northern Oman, Geophysical Journal International, 157, 381-398.

Walker, R. and Fattahi, M., 2011, A framework of Holocene and Late Pleistocene environmental change in eastern Iran inferred from the dating of periods of alluvial fan abandonment, river terracing, and lake deposition, Quaternary Science Reviews, 30(9-10), 1256-1271.

Walker, R. and Jackson, J., 2004, Active tectonics and late Cenozoic strain distribution in central and eastern Iran, Tectonics, 23, TC5010, 10.1029/2003TC001529.

Walker, R., Jackson, J., and Baker, C., 2004, Active faulting and seismicity of the Dasht-e-Bayaz region, eastern Iran, Geophysical Journal International, 157, 265-282.

Walker, R., Talebian, M., Sloan, R. A., Rasheedi, A., Fattahi, M. and Bryant, C., 2010, Holocene slip-rate on the Gowk strike-slip fault and implications for the distribution of tectonic strain in eastern Iran, Geophysical Journal International, doi:10.1111/j.1365-246X.2010.04538.x.